CORROSION BEHAVIOR OF 18% Ni M250 GRADE MARAGING STEEL UNDER WELD-AGED CONDITION IN SULFURIC ACID MEDIUM

B. S. Sanatkumar , Jagannath Nayak & A. Nityananda Shetty

Taylor & Francis
Taylor & Francis Group

Corrosion Behavior of 18% Ni M250 Grade Maraging Steel Under Weld-Aged Condition in Sulfuric Acid Medium

B. S. SANATKUMAR,[1] JAGANNATH NAYAK,[2] AND A. NITYANANDA SHETTY[1]

[1]Department of Chemistry, National Institute of Technology Karnataka, Surathkal, Srinivasnagar, Karnataka, India
[2]Department of Metallurgical and Materials Engineering, National Institute of Technology Karnataka, Surathkal, Srinivasnagar, Karnataka, India

The corrosion behavior of 18% Ni M250 grade maraging steel under weld-aged condition was investigated in sulfuric acid medium of different concentrations (0.1–2 M) at different temperatures (30°–60°C). Electrochemical measurements were carried out using the potentiodynamic polarization technique and electrochemical impedance spectroscopy (EIS). The results showed an increase in the corrosion rate with the increases in temperature as well with increase in the concentration of the corrosion medium. The results obtained from the Tafel extrapolation technique and electrochemical impedance spectroscopy were in good agreement. Activation parameters were evaluated using the Arrhenius equation and transition state equation. The surface morphology of the corroded specimen was compared with that of the un-corroded sample by using scanning electron microscopy (SEM).

Keywords Corrosion; EIS; Maraging steel; Polarization; SEM; Sulfuric acid

Introduction

Maraging steels are a class of ultrahigh-strength steels developed mainly for aerospace, aircraft, and tooling applications. The term *maraging* derives from martensite aging, referring to the heat treatment carried out to induce the precipitation of intermetallics in the Fe-Ni martensitic matrix, responsible for excellent mechanical properties. Aging is carried out in the range 400°–550°C, and a prolonged exposure above 500°C causes the reversion of martensite to austenite, which leads to over-aging (Menapace et al., 2010). The size and type of the intermetallic precipitates depend upon both the alloy composition and the applied aging treatment (Schnitzer et al., 2010). Maraging steels were developed in 1960s for applications requiring ultrahigh strength in combination with good fracture toughness. The alloys are low carbon steels that classically contain about 18 wt.% Ni, substantial amounts

of Co and Mo, together with small additions of Ti. However, depending on the requirements of the application, the composition of the material can be modified (Stiller et al., 1996). These steels are well known for their high strength, hardness and fracture toughness, high yield point and high strength at elevated temperature, and high resistance to thermo-mechanical fatigue. These steels also show good weldability, easy machinability, and good dimensional stability. Because of this unique combination of numerous attractive properties, the use of maraging steels has been extended to numerous areas of industrial applications such as the aerospace, nuclear, automobile, and marine industries (Grum and Slabe, 2006). For many of the applications of maraging steels, welding is the important means of fabrication. The unique property of being weldable in the solutionized condition followed by a low-temperature (480°C) post-weld maraging treatment makes these steels attractive for fabrication of large structures (Adama and Travis, 1964). They frequently come into contact with acids during processes such as cleaning, pickling, de-scaling, and acidizing. Therefore, studying the corrosion behavior of maraging steel under weld-aged condition is important.

A few research reports in the literature reveal that 18% Ni M250 grade maraging steel undergoes rusting easily in humid atmospheres and its rate of corrosion is quite high in acidic environments. The influence of phosphoric acid on the corrosion of aged and annealed 18 Ni 250 grade maraging steel has been investigated by Poornima et al. (2010). Krick et al. (1968) have reported the uniform corrosion of 18 Ni maraging steel when it was exposed to an open atmosphere. The effect of carbonate ions in slightly alkaline medium on the corrosion of maraging steel was studied by Bellanger (1994). Bellanger and Rameau (1996) studied the effect of slightly acidic pH with or without chloride in radioactive water on the corrosion of maraging steel and reported that corrosion behavior of maraging steel at the corrosion potential depends on pH and on the intermediated remaining on the maraging steel surface in the active region, favoring passivity. Maraging steels are found to be less susceptible to hydrogen embrittlement than common high-strength steels owing to the significantly low diffusion of hydrogen in these steels (Rezek et al., 1997). Corrosion rate and passive current density have been reported to increase as the structure is varied from fully annealed to fully aged on heat treatment (Poornima et al., 2010). Poornima et al. (2011) have reported the results of studies on the inhibition effect of 3,4-dimethoxybenzaldehydethiosemicarbazone on the corrosion of aged maraging steel in 0.5 M sulfuric acid. Although extensive work has been carried out on different properties of maraging steel through microstructure characterization, no significant work has been reported on studies of corrosion behavior of weld-aged maraging steel. In this investigation an attempt has been made to study the corrosion behavior of weld-aged maraging steel in different concentrations of H_2SO_4 at different temperatures.

Experimental Section

Material

The experiments were performed with specimens of weld-aged maraging steel (18% Ni M250 grade). The percentage composition of 18% Ni M250 grade maraging steel sample is given in Table I. Maraging steel plates with the composition given in Table I were welded by gas tungsten arc welding (GTAW) technique using a direct

Table I. Composition of the specimen (% by weight)

Element	Composition	Element	Composition
C	0.015%	Ti	0.3–0.6%
Ni	17–19%	Al	0.005–0.15%
Mo	4.6–5.2%	Mn	0.1%
Co	7–8.5%	P	0.01%
Si	0.1%	S	0.01%
O	30 ppm	N	30 ppm
H	2.0 ppm	Fe	Balance

current straight polarity (DCSP) with five passes, using filler material with the composition given in Table II. A specimen was taken from all the weld regions of the maraging steel plates that were welded as per above and aged at $480 \pm 5°C$ for 3 h, followed by air cooling.

Preparation of Test Coupons

Cylindrical test coupons were cut from the plate and sealed with epoxy resin in such a way that the area exposed to the medium was $0.64 \, cm^2$. These coupons were polished mechanically using emery papers of grades 180, 400, 600, 800, 1000, 1500, and 2000, then on a polishing wheel using legated alumina to obtain a mirror finish, washed thoroughly with double-distilled water, and degreased with acetone before being immersed in the acid solution.

Medium

Standard solutions of sulfuric acid having concentrations of 0.1, 0.5, 1, 1.5, and 2 M were prepared by diluting analytical grade sulfuric acid with double-distilled water. Experiments were carried out using a calibrated thermostat at temperatures of 30°, 40°, 50°, and 60°C ($\pm 0.5°C$).

Electrochemical Measurements

For electrochemical measurements the arrangement used was a conventional three-electrode compartment glass cell with a platinum counter electrode and a saturated calomel electrode (SCE) as reference. The working electrodes were made of

Table II. Composition of the filler material used for welding (% by weight)

Element	Composition	Element	Composition
C	0.015%	Ti	0.015%
Ni	17%	Al	0.4%
Mo	2.55%	Mn	0.1%
Co	12%	Si	0.1%
Fe	Balance		

weld-aged maraging steel. Electrochemical measurements were carried out by using an electrochemical workstation, Gill AC, using ACM Instruments Version 5 software. Electrode potentials were measured with respect to a saturated calomel electrode (SCE). The polarization studies were done immediately after the EIS studies on the same electrode without any further surface treatment.

Tafel Polarization Studies

Finely polished weld-aged maraging steel specimens of $0.64\,cm^2$ surface area were exposed to corrosion media of different concentrations of sulfuric acid (0.1–2 M) at different temperatures (30°–60°C), and the open circuit potential (OCP) was recorded until a steady-state open circuit potential was registered. The mean value of the readings corresponding to the last 5 min is taken as the open circuit potential. The potentiodynamic current potential curves were recorded by polarizing the specimen to $-250\,mV$ cathodically and $+250\,mV$ anodically with respect to OCP at a scan rate of $1\,mV\,s^{-1}$.

Electrochemical Impedance Spectroscopy Studies (EIS)

The electrochemical impedance spectra (EIS) were obtained in the frequency range of 10^3 to $10^{-2}\,Hz$ at the OCP by applying $10\,mV$ sine wave AC voltage, and the impedance data were analyzed using Nyquist plots. The double-layer capacitance (C_{dl}) and the charge transfer resistance (R_{ct}) were determined from the diameters of the semicircular Nyquist plots using the circle fit method. The number of data measured in each of the EIS experimental trials is 50.

In all the above measurements, at least three similar results were considered, and their average values are reported.

Scanning Electron Microscopy (SEM)

The surface morphology of the weld-aged maraging steel specimen immersed in sulfuric acid solution was compared with that of the noncorroded element using a JEOL JSM-6380LA analytical scanning electron microscopy. SEM images of corroded specimens were recorded without any further surface treatment. Energy dispersive spectroscopy (EDS) profiles on the surfaces of the noncorroded and corroded specimens were also recorded using the same instrument.

Results and Discussion

Tafel Polarization Measurements

The effect of sulfuric acid concentration on the corrosion rate of weld-aged samples of maraging steel was studied using the Tafel polarization technique. Figure 1 presents the potentiodynamic polarization curves for the corrosion of weld-aged samples of maraging steel in sulfuric acid solutions of different concentrations at 30°C. Similar plots were also obtained at other temperatures. The electrochemical parameters including corrosion potential (E_{corr}), corrosion current (i_{corr}), corrosion rate (v_{corr}), and anodic and cathodic slopes (b_a and b_c) were calculated from Tafel plots and are summarized in Table III. The corrosion current density (i_{corr}) increases
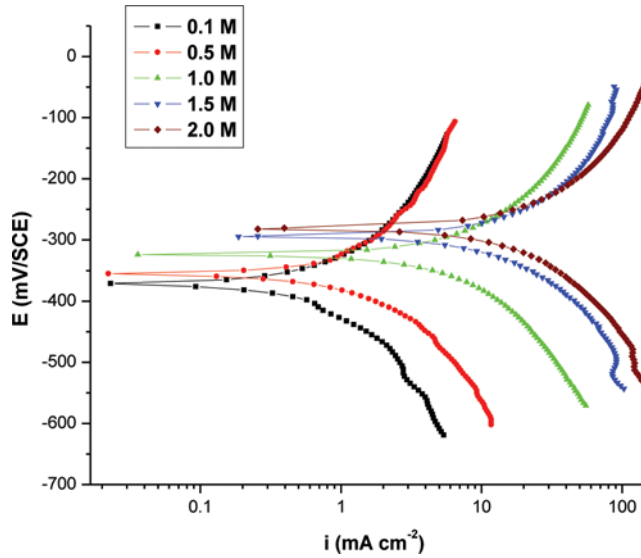
Figure 1. Potentiodynamic polarization curves for the corrosion of weld-aged maraging steel in different concentrations of sulfuric acid at 30°C. (Figure provided in color online.)

Table III. Electrochemical polarization parameters for the corrosion of weld-aged maraging steel in different concentrations of sulfuric acid at different temperatures

Concentration of H_2SO_4 (M)	Temperature T (K)	E_{corr} (mV vs SCE)	b_a (mV dec^{-1})	$-b_c$ (mV dec^{-1})	i_{corr} (mA cm^{-2})	v_{corr} (mm y^{-1})
0.1	303	−371	221	266	0.78	8
	313	−371	289	365	1.99	20
	323	−373	298	321	2.47	25
	333	−351	333	343	4.26	43
0.5	303	−356	335	268	1.80	18
	313	−354	293	281	3.83	39
	323	−351	287	274	4.30	43
	333	−350	307	363	4.62	46
1	303	−323	247	301	8.56	86
	313	−309	312	311	16.9	170
	323	−305	292	307	22.00	222
	333	−302	283	305	24.00	244
1.5	303	−295	252	260	17.00	178
	313	−288	254	283	28.00	282
	323	−283	272	266	33.00	339
	333	−276	296	306	36.00	362
2	303	−281	223	251	20.00	205
	313	−278	269	274	35.00	356
	323	−273	301	302	45.00	459
	333	−264	330	322	61.00	623

with increase in the concentration of sulfuric acid in the solution, indicating an increase in the corrosion rate with the increase in sulfuric acid concentration. Although the values of b_c and b_a change with the increase in acid concentration, there is no definite trend observed for the change. This indicates the influence of acid concentration on the kinetics of hydrogen evolution and metal dissolution.
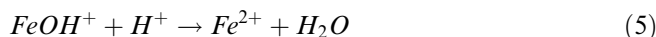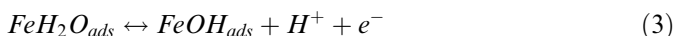
The corrosion rate is calculated using:

$$v_{corr}\left(\text{mmy}^{-1}\right) = \frac{3270 \times EW \times i_{corr}}{\rho} \tag{1}$$

where 3270 is a constant that defines the unit of corrosion rate, i_{corr} is the corrosion current density in A cm^{-2}, ρ is the density of the corroding material (8.23 g cm^{-3}) and EW is the equivalent weight of the alloy (Fontana, 1987). The equivalent weight is given by the expression:

$$EW = \frac{1}{\Sigma \frac{n_i f_i}{W_i}} \tag{2}$$

where f_i is the mass fraction of the ith element in the alloy, W_i is the atomic weight of the ith element in the alloy, and n_i is the valence of the ith element of the alloy. The corrosion current density (i_{corr}) is obtained by extrapolating the anodic and cathodic Tafel regions on the polarization curves to intersect at the corrosion current density.

It is observed from these results that the corrosion rate of the weld-aged maraging steel increases with the increase in sulfuric acid concentration in the solution. It is also evident from Figure 1 and Table III that the corrosion potential (E_{corr}) is shifted towards less negative values as the concentration of sulfuric acid is increased. It is also seen from Figure 1 that both the anodic and cathodic polarization curves are shifted with the increase in sulfuric acid concentration, which result in the positive shift of E_{corr} values. The shift appears to be relatively more for the cathodic branch than for the anodic branch. Thus both the anodic and cathodic processes are affected by the increase in acid concentration. The following consecutive mechanism is proposed for the anodic dissolution of iron in sulfuric acid medium (Bockris et al., 1963):

$$FeH_2O_{ads} \leftrightarrow FeOH_{ads} + H^+ + e^- \tag{3}$$

$$FeOH_{ads} \rightarrow FeOH^+ + e^- \tag{4}$$

$$FeOH^+ + H^+ \rightarrow Fe^{2+} + H_2O \tag{5}$$

Iron electro dissolution in acidic sulfate solution depends primarily on the adsorbed intermediate FeOH$_{ads}$ as per the above mechanism.

The following stages are possible for the hydrogen evolution reaction on iron (Devanathan and Stachurski, 1964):

$$Fe + H^+ + e^- \rightarrow FeH \tag{6}$$

$$FeH + FeH \rightarrow 2Fe + H_2 \tag{7}$$

$$FeH + H^+ + e^- \rightarrow Fe + H_2 \tag{8}$$
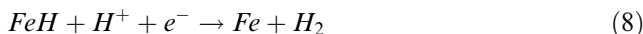
The overall chemical reaction is the sum of these two half-cell reactions:

$$Fe + 2H^+ \rightarrow Fe^{2+} + H_2 \uparrow \tag{9}$$

The corrosion rate of iron in sulfuric acid is controlled by both hydrogen evolution reaction and iron dissolution.

Electrochemical Impedance Spectroscopy

Nyquist plots for the corrosion of weld-aged maraging steel in different concentrations of H_2SO_4 at 30°C are shown in Figure 2, with the inset showing a zoom of the high-frequency region. Similar results were obtained at the other four temperatures. The similar semicircular appearance of the impedance diagrams shows that the corrosion of weld-aged maraging steel is controlled by a charge transfer process and the mechanism of dissolution of the metal is not affected by variation in the concentration of sulfuric acid (Larabi et al., 2005). The charge transfer resistance (R_{ct}) was evaluated from the diameter of the semicircle, which is inversely proportional to the corrosion current and was used to calculate the corrosion rate.

The corrosion current density i_{corr} was calculated using the Stern-Geary equation (El-Sayed, 1997):

$$i_{corr} = \frac{b_a b_c}{2.303(b_a + b_c)} \times \frac{1}{R_{ct}} \tag{10}$$
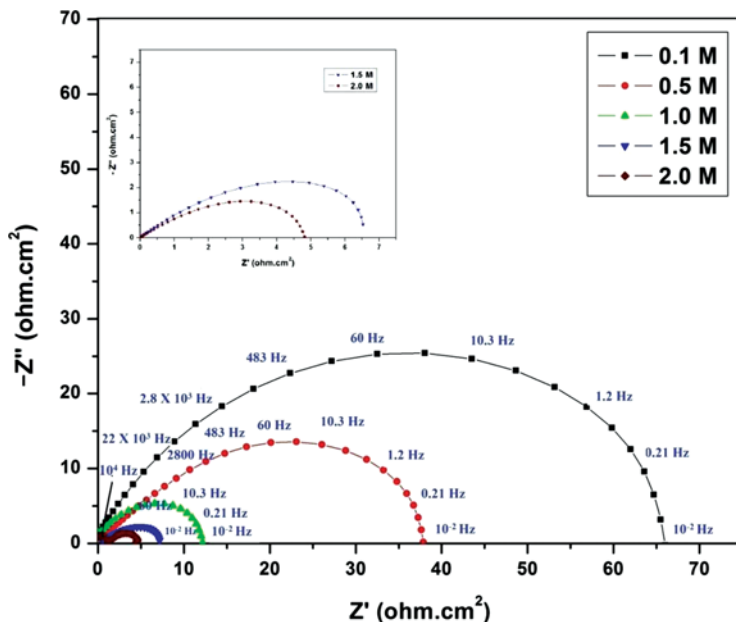
Figure 2. Nyquist plots for the corrosion of weld-aged maraging steel in different concentrations of sulfuric acid at 30°C. (Figure provided in color online.)

The results obtained can be interpreted in terms of the equivalent circuit of the electrical double layer shown in Figure 3, which has been used previously to model the iron/acid interface (Prabhu et al., 2008). The circuit fitting was done by ZSimpWin software, version 3.21. The equivalent circuit falls into the classical capacitor and resistor combination. The equivalent circuit consists of a parallel combination of charge-transfer resistance (R_{ct}) and constant phase element (CPE), both in series with the solution resistance (R_s). The CPE element is used as a substitute for the capacitor in Figure 3 to explain the depression of the capacitance semicircle, which corresponds to the surface heterogeneity resulting from such conditions as surface roughness, impurities, dislocations, grain boundaries, adsorption of ions, and formation of porous layers (Li et al., 2008). The CPE impedance (Z_{CPE}) is given by the expression:

$$Z_{CPE} = \frac{1}{Q} \times \frac{1}{(j\omega)^n} \tag{11}$$

where Q is the CPE coefficient, n is the CPE exponent (phase shift), ω is the angular frequency ($\omega = 2\pi f$, where f is the AC frequency), and j here is the imaginary unit ($j = (-1)^{1/2}$). When the value of n is 1, the CPE behaves like an ideal double-layer capacitance (C_{dl}). The correction of capacity to its real values is calculated from

$$C_{dl} = Q(\omega_{max})^{n-1} \tag{12}$$

where ω_{max} is the frequency at which the imaginary part of the impedance ($-Z_i$) has a maximum (Machnikova et al., 2008). The impedance parameters obtained are listed in Table IV. The results show that the charge transfer resistance (R_{ct}) values decrease with an increase in acid concentration. Also, the double-layer capacitance
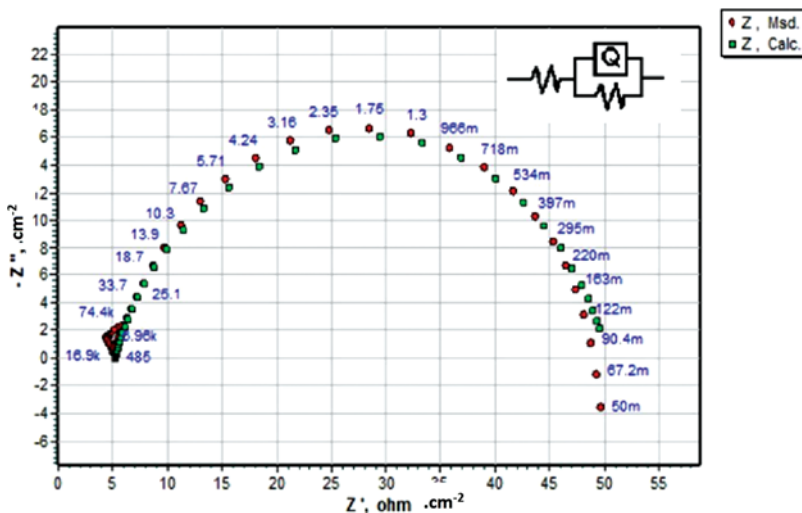

Figure 3. The equivalent circuit model used to fit the experimental data for the corrosion of weld-aged maraging steel in 0.1 M sulfuric acid at 40°C. (Figure provided in color online.)

Table IV. Electrochemical impedance parameters for the corrosion of weld-aged maraging steel in different concentrations of sulfuric acid at different temperatures

Concentration of H_2SO_4 (M)	Temperature (K)	C_{dl} ($\mu F\ cm^2$)	R_{ct} (Ωcm^2)	i_{corr} (mA cm^{-2})	v_{corr} (mm y^{-1})
0.1	303	2101	66.0	0.67	7
	313	3605	42.0	1.79	18
	323	4179	31.0	2.10	21
	333	6446	22.0	3.98	40
0.5	303	4012	38.0	1.56	16
	313	10977	15.0	3.40	34
	323	15827	14.0	4.11	41
	333	21056	15.0	5.56	56
1	303	11000	12.0	7.40	74
	313	12370	5.0	16.5	166
	323	18083	4.0	17.6	177
	333	23000	3.5	20.1	202
1.5	303	13700	5.0	16.3	164
	313	14040	2.1	28.1	282
	323	21000	1.8	33.2	333
	333	27625	1.8	35.4	353
2	303	16400	3.0	20.9	210
	313	17569	1.7	33.7	339
	323	26003	1.4	45.2	454
	333	37000	1.2	60.3	605

(C_{dl}) increases with an increase in the concentration of the acid solution. Both the factors indicate an increase in the corrosion rate of the alloy with an increase in the concentration of sulfuric acid. This is in accordance with the observations obtained from potentiodynamic measurements.
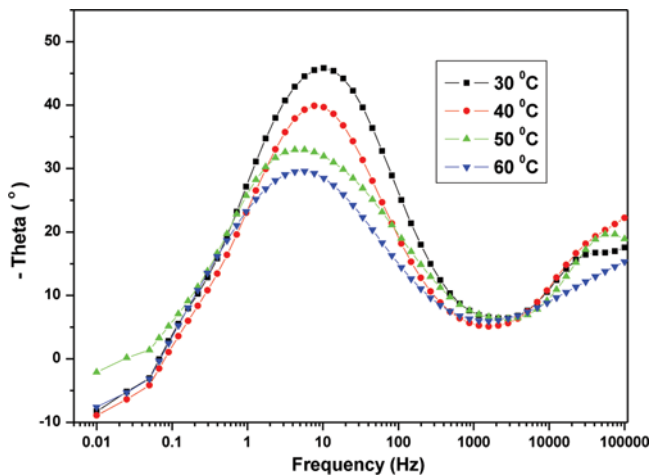
Figures 4 and 5 represent the Bode phase plots for the corrosion of weld-aged maraging steel in sulfuric acid solutions of different concentrations at 30°C and in 0.1 M sulfuric acid at different temperatures, respectively. The Bode plots show only one capacitive time constant. The high frequency (HF) part of the impedance and phase angle describes the behavior of an inhomogeneous surface layer, while the low frequency (LF) contribution shows the kinetic response for the charge transfer reaction (Khaled and Hackerman, 2003). As described in the mechanism of iron dissolution, the adsorbed layer of the intermediate $FeOH_{ads}$ controls the charge transfer at the metal/solution interface. The high frequency limits correspond to $R_s(\Omega)$, while the low frequency limits correspond to ($R_s + R_{ct}$), which is associated with the dissolution processes at the interface. It can be seen from Figures 4 and 5 that the phase angle decreases with an increase in the concentration of sulfuric acid, indicating a decrease in capacitive behavior at the interface due to the continuous and increased metal dissolution. It is also seen that the difference between the HF and LF for the corroded system in the Bode plot decreases with an increase in the concentration of sulfuric acid, indicating a decrease in charge transfer resistance (R_{ct}) and increase in the corrosion rate.
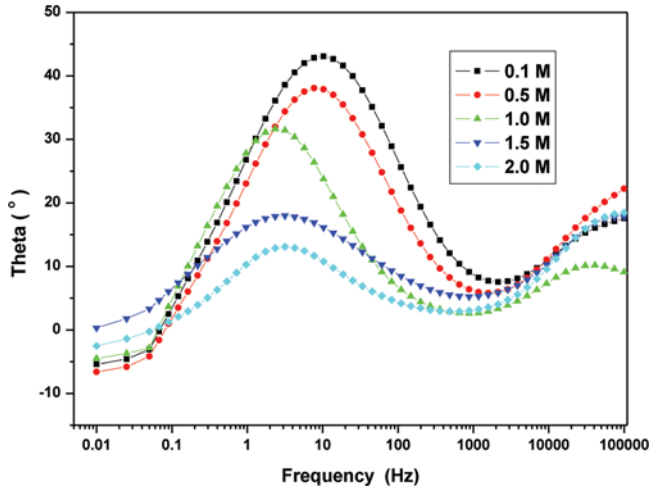
Figure 4. Bode phase plots for the corrosion of weld-aged maraging steel in different concentrations of sulfuric acid at 30°C. (Figure provided in color online.)

Effect of Temperature

The effect of temperature on the corrosion rate of weld-aged maraging steel was studied by measuring the corrosion rates at different temperature between 30° and 60°C. Figures 6 and 7 represent the potentiodynamic polarization curves and Nyquist plots, respectively, at different temperatures for the corrosion of weld-aged maraging steel samples in 1 M H$_2$SO$_4$ solution. Similar plots were obtained in other concentrations of the solutions. The Tafel polarization results and EIS results pertaining to the corrosion of the alloy at different temperatures are listed in Tables III and IV, respectively. It is clear from the data presented in the tables that
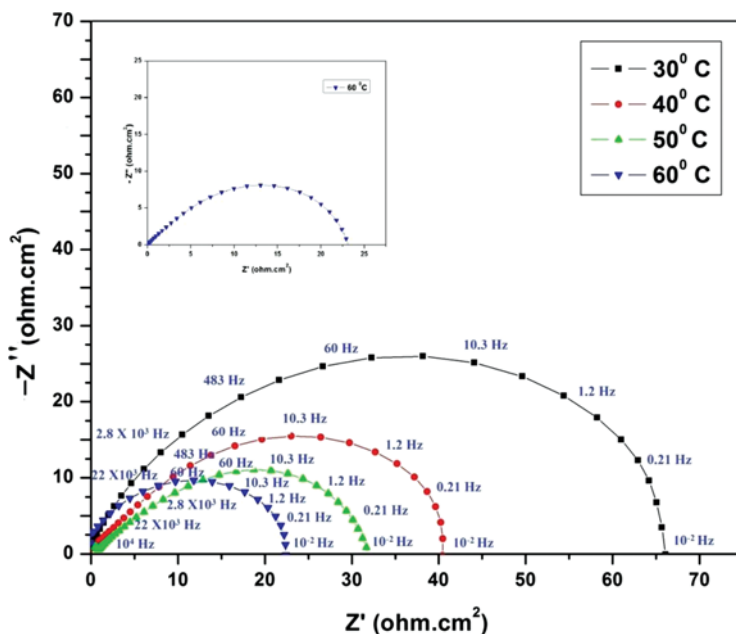

Figure 5. Bode phase plots for the corrosion of weld-aged maraging steel in 0.1 M sulfuric at different temperatures. (Figure provided in color online.)
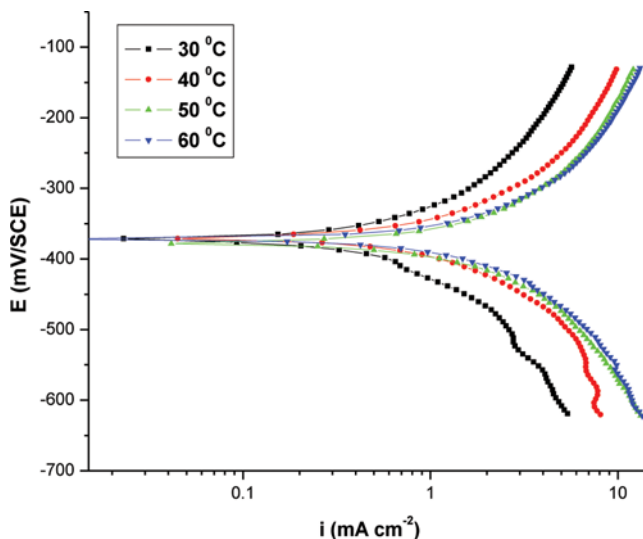
Figure 6. Potentiodynamic polarization curves for the corrosion of weld-aged maraging steel at different temperatures in 0.1 M sulfuric acid. (Figure provided in color online.)

the corrosion rate of weld-aged maraging steel increases with an increase in the temperature of sulfuric acid medium. This may be attributed to the fact that the hydrogen evolution over potential decreases with increase in temperature, which leads to increase in cathodic reaction rate (Bellanger and Rameau, 1996), in turn increasing the rate of overall corrosion reaction.

Figure 7. Nyquist plots for the corrosion of weld-aged maraging steel at different temperatures in 0.1 M sulfuric acid. (Figure provided in color online.)
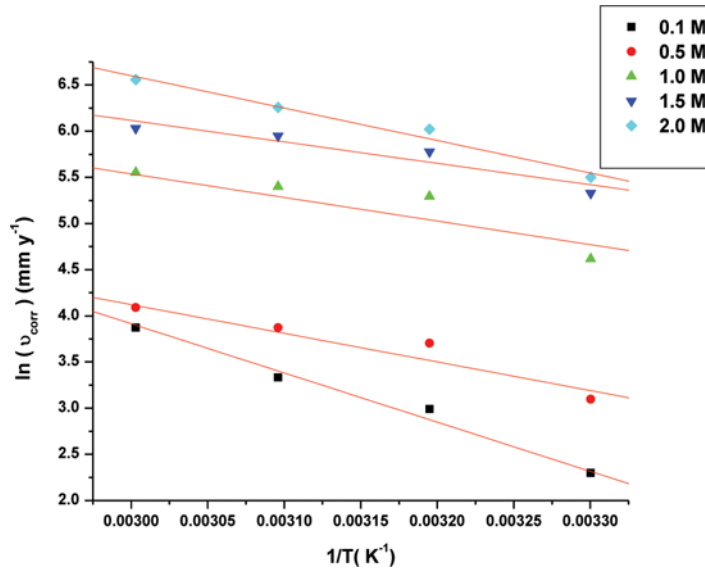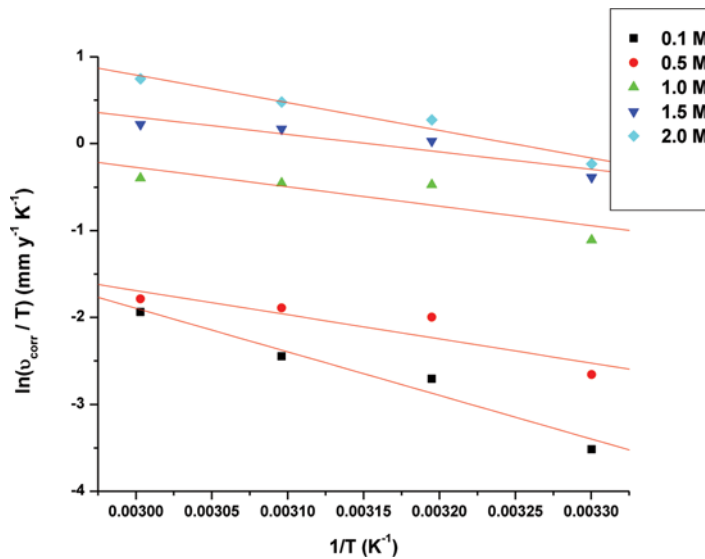
Figure 8. Arrhenius plots for the corrosion of weld-aged maraging steel in sulfuric acid. (Figure provided in color online.)

The value of activation energy (E_a) was calculated from the Arrhenius equation:

$$\ln(\upsilon_{corr}) = B - (E_a/RT) \tag{13}$$

where B is a constant that depends on the metal type, R is the universal gas constant, and T is the absolute temperature. A plot of $\ln(\upsilon_{corr})$ versus $1/T$ gives a straight line

Figure 9. $\ln(\upsilon_{corr}/\ T)$ vs. $1/T$ plots for the corrosion of weld-aged maraging steel in sulfuric acid. (Figure provided in color online.)

Table V. Activation parameters of corrosion reaction of weld-aged maraging steel specimens in sulfuric acid

Concentration of H_2SO_4 (M)	E_a (kJ mol^{-1})	$\Delta H^{\#}$ (kJ mol^{-1})	$\Delta S^{\#}$ (J mol^{-1} K^{-1})
0.1	44.31	44.16	−88.32
0.5	29.79	26.48	−111.52
1	25.79	23.11	−144.08
1.5	19.29	16.69	−144.93
2	21.20	18.58	−142.28

with a slope of $-E_a$/R. The Arrhenius plots for the corrosion of weld-aged specimens in sulfuric acid are shown in Figure 8.

The enthalpy of activation ($\Delta H^{\#}$) and entropy of activation ($\Delta S^{\#}$) values for the corrosion process were calculated from the transition state theory equation (Larabi et al., 2005):

$$v_{corr} = (RT/nh) \exp(\Delta S^{\#}/R) \exp(-\Delta H^{\#}/RT) \tag{14}$$

where h is Planck's constant, and N is Avogadro's number. A plot of $\ln(v_{corr}/T)$ versus $1/T$ gives a straight line with a slope of $-\Delta H^{\#}/R$ and an intercept of $\ln(R/Nh) + \Delta S^{\#}/R$. The plots of $\ln(v_{corr}/T)$ versus $1/T$ for the corrosion of weld-aged samples of maraging steel in different concentrations of sulfuric acid are shown in Figure 9. The activation parameters calculated are listed in Table V. The activation energy (E_a) values indicate that the corrosion of the alloy is controlled by surface reaction, since the values of activation energy for the corrosion process
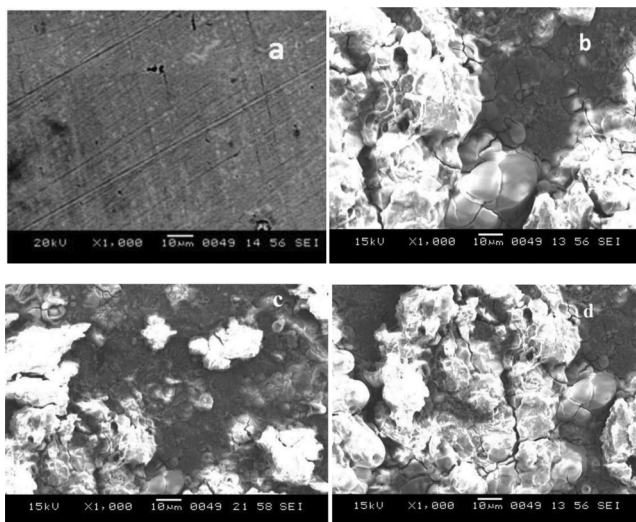
Figure 10. SEM images of (a) freshly polished surface of weld-aged maraging steel and after immersion for 3 h in (b) 2.0 M sulfuric acid, (c) 1.5 M sulfuric acid, and (d) 1.0 M sulfuric acid.

are greater than $20\,kJ\,mol^{-1}$ (Bouklah et al., 2005). Further, the activation energy values are lower than $30\,kJ\,mol^{-1}$ except when in 0.1 M sulfuric acid, indicating that the reactions at the surface of the alloy are predominantly diffusion controlled. It is also observed that activation energy value decreases with an increase in the concentration of sulfuric acid. As the concentration of the acid increases, the concentration of H^+ ions increases and in turn these ions can diffuse faster to the cathodic surface to take part in the cathodic reaction, as per Equations (6) and (8), and thereby increase the rate of cathodic reaction. The increased cathodic reaction induces an increase in the overall corrosion reaction. Thus, the activation energy for the corrosion process decreases and the corrosion rate increases as the acid concentration is increased.

The entropy of activation $\Delta S^{\#}$ is negative. This implies that the activated complex in the rate-determining step represents association rather than dissociation,
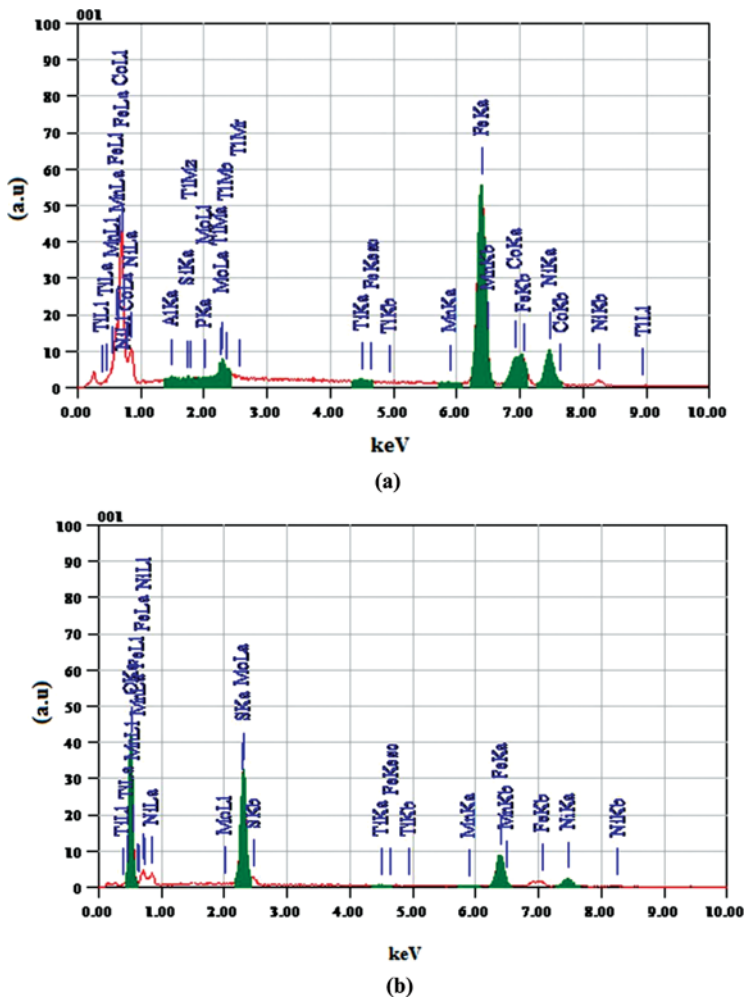
Figure 11. EDS profile on the surface of (a) freshly polished surface of weld-aged maraging steel and (b) after immersion for 3 h in 2.0 M sulfuric acid. (Figure provided in color online.)

resulting in a decrease in randomness taking place on going from the reactants to the activated complex (Abd Ei-Rehim et al., 1999).

Scanning Electron Microscopy (SEM)

The surface morphology of the weld-aged maraging steel specimens immersed in sulfuric acid solution was compared with that of the noncorroded element by recording their SEM images. The SEM image of a freshly polished surface of the weld-aged maraging steel sample is given in Figure 10(a), which shows the noncorroded surface with a few scratches due to polishing. Figures 10(b), 10(c), and 10(d) show, respectively, the SEM images of weld-aged maraging steel surfaces after immersion for 3 h in 2.0, 1.0, and 0.5 M sulfuric acid. The SEM images reveal that the specimens undergo severe corrosion in the sulfuric acid solution. As the concentration of sulfuric acid increases, the extent of corrosion also increases. Elemental analysis using SEM/EDS is useful for qualitative and semi-quantitative determination of elemental content and for obtaining correlation between microstructures and elemental composition. The EDS profile of the noncorroded and corroded surface of the alloy samples are presented in Figures 11(a) and 11(b), respectively. The EDS profile of the noncorroded sample (Figure 11(a)) shows peaks corresponding to Fe, Ni, Mo, and Ti. Additional peaks corresponding to O, S, and Co are seen in the EDS profile of the corroded specimen (Figure 11(b)). In addition to the above, it is also seen that iron content on the surface decreased, whereas Ni content increased. The above facts indicate the presence of oxides and sulfates of Fe, Co, and Ni on the surface of the alloy. The ions of Fe, Co, and Ni formed due to the anodic dissolution of the alloy combine with the oxide and sulfate ions, resulting in the formation of oxides and sulfates on the alloy surface.

Conclusions

Based on the results of investigation, the following conclusions are drawn:

1. The corrosion rate of the weld-aged maraging steel specimens in sulfuric acid medium is substantial.
2. The potentiodynamic polarization and impedance studies showed that the corrosion rate of the specimen is influenced by temperature and concentration of sulfuric acid. The corrosion rate increases with an increase in the concentration of H_2SO_4 and also with an increase in temperature.
3. The anodic dissolution of the alloy takes place through a consecutive mechanism, with the formation of $FeOH_{ads}$ intermediate. The adsorbed layer of the intermediate $FeOH_{ads}$ controls the charge transfer at the metal/solution interface. Hydrogen liberation is the cathodic reacation.
4. The corrosion rates determined by potentiodynamic polarization and EIS are in reasonably good agreement.
5. The corrosion kinetics follows the Arrhenius law.

References

Abd Ei-Rehim, S. S., Ibrahim, M. A. M., and Khaled, K. F. (1999). 4-Aminoantipyrine as an inhibitor of mild steel corrosion in HCl solution, *J. Appl. Electrochem.*, **29**, 595–599.

Adama, C. M., and Travis, R. E. (1964). Welding of 18% Ni-Co-Mo maraging alloys, *Weld. J.*, **43**, 193–197.

Bellanger, G. (1994). Effect of carbonate in slightly alkaline medium on the corrosion of maraging steel, *J. Nucl. Mater.*, **217**, 187–193.

Bellanger, G., and Rameau, J. J. (1996). Effect of slightly acid pH with or without chloride in radioactive water on the corrosion of maraging steel, *J. Nucl. Mater.*, **228**, 24–37.

Bockris, J. O. M., Devanathan, M. A., and Muller, K. (1963). On structures of charged interfaces, *Proc. Roy. Soc. A*, **274**, 55–79.

Bouklah, M., Hammouti, B., Benkaddour, M., and Benhadda, T. (2005). Thiophene derivatives as effective inhibitors for the corrosion of steel in $0.5\,M\ H_2SO_4$, *J. Appl. Electrochem.*, **35**, 1095–1101.

Devanathan, M. A., and Stachurski, Z. (1964). The mechanism of hydrogen evolution on iron in acid solutions by determination of permeation rates, *J. Electrochem. Soc.*, **111**, 619–620.

El-Sayed, A. (1997). Phenothiazine as inhibitor of the corrosion of cadmium in acidic solutions, *J. Appl. Electrochem.*, **27**, 193–200.

Fontana, M. G. (1987). *Corrosion Engineering*, 3rd ed., McGraw-Hill, Singapore.

Grum, J., and Slabe, J. M. (2006). Effect of laser-remelting of surface cracks on microstructure and residual stresses in 12Ni maraging steel, *Appl. Surf. Sci.*, **252**, 4486–4492.

Khaled, K. F., and Hackerman, N. (2003). Investigation of the inhibitive effect of ortho-substituted anilines on corrosion of iron in $0.5\,H_2SO_4$ solutions, *Mater. Chem. Phys.*, **82**, 949–960.

Krick, W. W., Covert, R. A., and May, T. P. (1968). Corrosion behavior of high strength steels in marine environment, *Met. Eng. Q.*, **8**, 31.

Larabi, L., Harek, Y., Benali, O., and Ghalem, S. (2005). Hydrazide derivatives as corrosion inhibitors for mild steel in 1 M HCl, *Prog. Org. Coat.*, **54**, 256–262.

Li, W.-H., He, Q., Zhang, S.-T., Pei, C.-P., and Hou, B.-R. (2008). Some new triazole derivatives as inhibitors for mild steel corrosion in acidic medium, *J. Appl. Electrochem.*, **38**, 289–295.

Machnikova, E., Kenton, W. H., and Hackerman, N. (2008). Corrosion inhibition of carbon steel in hydrochloric acid by furan derivatives, *Electrochim. Acta*, **53**, 6024–6032.

Menapace, C., Lonardelli, I., and Molinari, A. (2010). Phase transformation in a nanostructured M300 maraging steel obtained by SPS of mechanically alloyed powders, *J. Therm. Anal. Calorim.*, **101**, 815–821.

Poornima, T., Nayak, J., and Shetty, A. N. (2010). Corrosion of aged and annealed 18 Ni 250 grade maraging steel in phosphoric acid medium, *Int. J. Electrochem. Sci.*, **5**, 56–71.

Poornima, T., Nayak, J., and Shetty, A. N. (2011). 3,4-Dimethoxybenzaldehyde thiosemicarbazone as corrosion inhibitor for aged 18Ni 250 grade maraging steel in 0.5 M sulfuric acid, *J. Appl. Electrochem.*, **41**, 223–233.

Prabhu, R. A., Shanbhag, A. V., and Venkatesha, T. V. (2007). Influence of tramadol [2-[(dimethylamino)methyl]-1-(3-methoxyphenyl) cyclohexanol hydrate] on corrosion inhibition of mild steel in acidic media, *J. Appl. Electrochem.*, **37**, 491–497.

Prabhu, R. A., Venkatesha, T. V., Shanbhag, A. V., Kulkarni, G. M., and Kalkhambkar, R. G. (2008). Inhibition effects of some Schiff's bases on the corrosion of mild steel in hydrochloric acid solution, *Corros. Sci.*, **50**, 3356–3362.

Rezek, J., Klein, I. E., and Yhalom, J. (1997). Structure and corrosion resistance of oxides grown on maraging steel in steam at elevated temperatures, *Appl. Surf. Sci.*, **108**, 159–167.

Schnitzer, R., Schober, M., Zinner, S., and Leitner, H. (2010). Effect of Cu on the evolution of precipitation in an Fe–Cr–Ni–Al–Ti maraging steel, *Acta Mater.*, **58**, 3733–3741.

Stiller, K., Danoix, F., and Bostel, A. (1996). Investigation of precipitation in a new maraging stainless steel, *Appl. Surf. Sci.*, **94–95**, 326–333.